A Zn(II)-binding site engineered into retinol-binding protein exhibits metal-ion specificity and allows highly efficient affinity purification with a newly designed metal ligand

André M Schmidt, Holger N Müller* and Arne Skerra

Background: The Zn(II)-binding site from the active center of human carbonic anhydrase II, formed by three His side chains, can be grafted onto the recombinant serum retinol-binding protein (RBP). The artificial binding site in the resulting variant RBP/H_3(A) has high affinity for Zn(II) and stabilizes the protein against denaturation.

Results: The metal-ion specificity of the grafted Zn(II) binding site in RBP/H_3(A) was investigated. Both Cu(II) and Ni(II) bound with high affinity, although the K_d values were not as low as for Zn(II) binding. Competition experiments with the chelate ligands iminodiacetic acid (IDA) and nitrilotriacetic acid (NTA) suggested that both Ni(II) and Cu(II) bound to the protein in an octahedral manner with three vacant coordination sites, as previously observed for Zn(II). A substituted pyrrolidine-dicarboxylic acid was designed as a structurally rigid IDA compound and coupled to a matrix. Using this support in an immobilized metal affinity chromatography (IMAC), RBP/H_3(A) was purified from the bacterial cell extract in one step with unprecedented efficiency.

Conclusions: Although the His_3 metal-binding site used here had been removed from the substrate pocket of an enzyme and exposed to solvent on a protein surface, it showed clear selectivity for Zn(II) compared to Cu(II) and Ni(II). Thus the properties of this structurally defined metal-binding site (which are not shared by isolated His residues or flexible oligo-His tags) can be preserved when it is added to proteins. An IMAC matrix with improved behavior was designed, allowing highly selective purification of RBP/H_3(A) and of His_6-tagged RBP as well. Such rational design of supramolecular recognition may be generally useful in the fields of protein engineering and drug design.

Address: Institut für Biochemie, Technische Hochschule, Petersenstr. 22, D-64287 Darmstadt, Germany.

*Present address: Biometra GmbH, Rudolf-Wissell-Str. 30, D-37079 Göttingen, Germany.

Correspondence: Arne Skerra
e-mail: di34@hrzpub.th-darmstadt.de

Key words: chelate ligand, equilibrium dialysis, immobilized metal affinity chromatography, lipocalin, protein design

Received: **10 Jun 1996**
Revisions requested: **8 Jul 1996**
Revisions received: **15 Jul 1996**
Accepted: **16 Jul 1996**

Chemistry & Biology August 1996, **3**:645–653

Introduction

The increase in knowledge about protein structure, function and stability in the past years has generated interest in the idea of designing artificial proteins with novel properties. As an alternative to the complex and as yet poorly understood process of constructing proteins *de novo*, one can try to introduce new functions into naturally existing proteins on the basis of their known crystallographic structure. The binding of ligands such as metal ions to proteins is an important prerequisite for a variety of biological activities, and several successful attempts to incorporate metal-binding sites into well-defined protein frameworks have been described (reviewed in [1]). Both α-helices and β-sheets have been used as templates for the introduction of the histidine and cysteine residues that formed the metal-binding sites. In both approaches, engineered metal-binding sites were found to either contribute to stabilization [2–4] or permit purification [5,6] of the protein.

Employing the biochemically [7] and structurally [8–10] well characterized retinol-binding protein (RBP) as a model system, the Zn(II)-binding site of human carbonic anhydrase II [11,12] was successfully transplanted [13]. The resulting protein, RBP/H_3(A) [13], was produced recombinantly in *Escherichia coli* [14,15]. It includes three newly introduced His residues on the outer surface of its β-barrel that, in order to enable the tight complexation of Zn(II), were placed in an environment with similar backbone structure as is present in carbonic anhydrase. The engineered binding site in RBP/H_3(A) was shown to exhibit high affinity for Zn(II) (K_d = 36 ± 10 nM) and to enhance the stability of the protein by 8.6 kJ mol^{-1} upon metal-complex formation [13].

As the His residues were exposed at the surface of the protein, it seemed possible that the metal-binding site could also be used for the purification of RBP/H_3(A) via immobilized metal affinity chromatography (IMAC) [16] and indeed, a separation of the recombinant protein from other host cell proteins could be achieved [13]. However, the selectivity was low, and carefully optimized conditions had to be used in conjunction with Ni(II) instead of Zn(II) as the complexing metal ion.

Figure 1

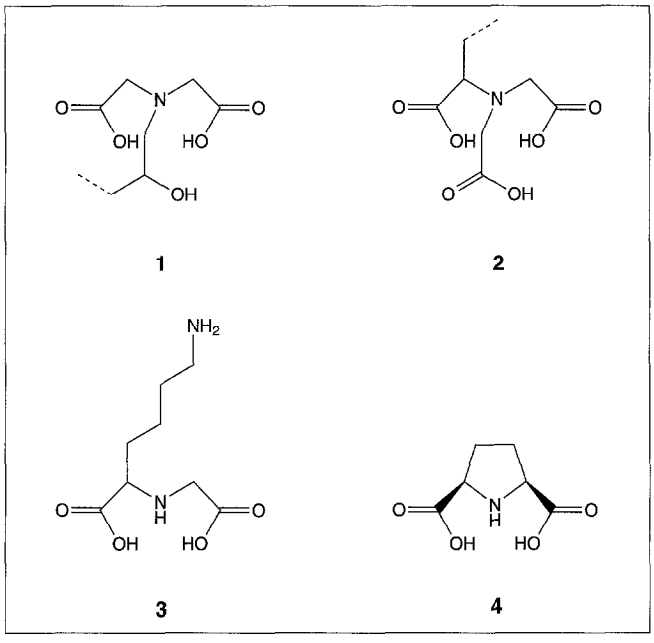

Chemical structures of iminodiacetic acid (IDA; compound **1**), nitrilotriacetic acid (NTA; compound **2**), N-carboxymethyl lysine (NCL; compound **3**) and pyrrolidine-(*R,S*)-dicarboxylic acid (PDC; compound **4**). IDA and NTA are shown in the configurations that result from coupling to the commercially available matrices [16,17] for better comparison of the functional groups that are involved in metal-ion complexation.

Generally, IMAC is based on metal chelate ligands such as iminodiacetic acid (IDA) or nitrilotriacetic acid (NTA), which are covalently attached to gel matrices in the form of their derivatives 1 and 2 [16,17] (Fig. 1). After charging these pseudo-affinity columns with transition-metal ions such as Cu(II), Ni(II), or Zn(II), proteins that display amino acid residues with metal complexing capability, mainly His sidechains, can be bound and subsequently eluted using an imidazole gradient. A fundamental problem in IMAC is that the affinity of the metal ion to the matrix must neither be too low, nor too high. Weak binding can lead to detachment of the metal ion by the protein from the matrix and thus loss of the purification effect. Strong binding, on the other hand, necessitates several chelating groups and results in a reduced number of coordination sites that remain for complex formation with the protein. An optimal interaction should therefore be achieved when the metal ion is bound between the chelate ligand of the matrix and the complexing amino acid sidechains of the protein in a 'sandwich'-like complex without competition for the metal center or steric hindrance. A similar concept was recently realised in the design of an interfacial Zn(II) binding site in a hormone–receptor complex [18].

In the present study we report the metal affinities of RBP/H_3(A) for Ni(II) and Cu(II) and we describe the construction of an advanced IMAC ligand that enables its highly selective purification using an optimal interaction as described above.

Results and discussion

Metal-binding affinities

As for Zn(II) binding [13], Cu(II)- and Ni(II)-binding properties of RBP/H_3(A) were determined in equilibrium

Figure 2

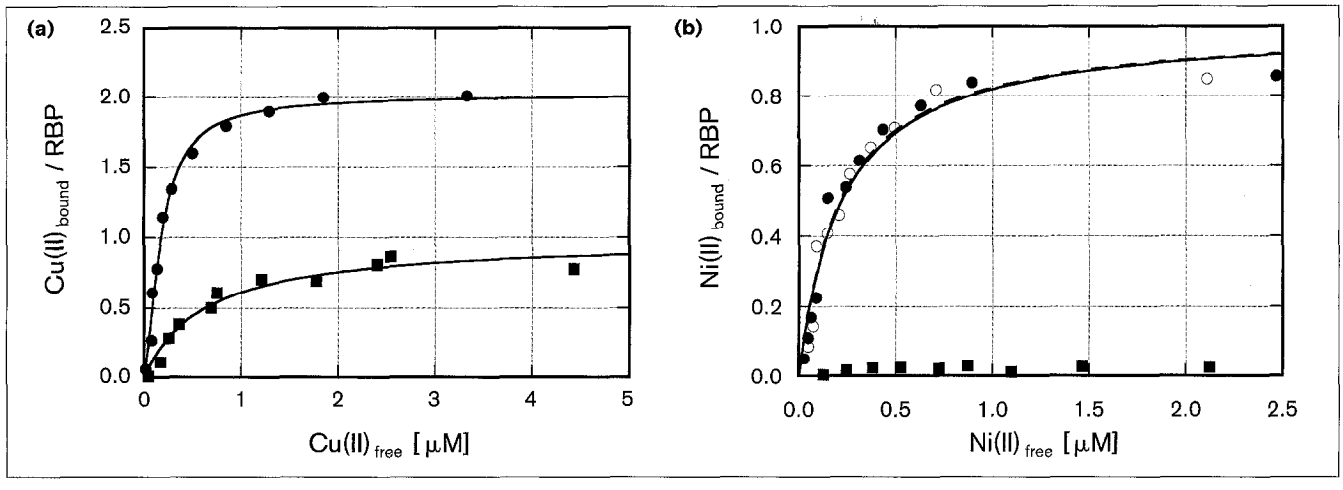

Metal-binding isotherms for RBP/H_3(A) from equilibrium dialysis experiments. The molar ratio of bound metal ion to protein is plotted against the concentration of free metal ion. The lines represent least-squares fits derived from equations described earlier [13]. The corresponding dissociation constants are given in Table 1. **(a)** Binding of Cu(II) to 2.8 μM RBP/H_3(A) (circles), or to 2.4 μM wild-type RBP (squares). Both measurements were performed in the presence of IDA. **(b)** Binding of Ni(II) to 4.5 μM RBP/H_3(A) in the absence (open circles, dashed line) or presence (filled circles, continuous line) of IDA, or to 3.8 μM wild-type RBP in the presence of IDA (squares).

Table 1

Metal affinities of RBP/H_3(A) based on equilibrium dialysis.

Metal ion	Stoichiometry	K_d (nM)
Zn(II)	1	36 ± 10[a]
Zn(II)-IDA[b]	1	44 ± 8[a]
Cu(II)-IDA	2[c]	292 ± 141; 111 ± 64
Ni(II)	1	224 ± 46
Ni(II)-IDA	1	217 ± 39

[a]Data from [13].
[b]IDA was present at 100 μM [13].
[c]The K_d for the single binding site in wild-type RBP was 612 ± 130 nM.

dialysis experiments using atomic absorption spectrometry for the quantification of protein-bound and free metal-ion concentrations. The metal ions were added either in uncomplexed (hydrated) form or in the presence of IDA or NTA. These metal chelate ligands were added in order to investigate whether the coordination sphere of the metal ion that was bound to RBP/H_3(A) allowed for the complexation of a further ligand. We observed that uncomplexed Cu(II) caused precipitation of the protein, so equilibrium dialysis with this transition-metal ion yielded useful data only in the presence of IDA.

RBP/H_3(A) exhibited quite similar affinities for Cu(II)-IDA, Ni(II), and Ni(II)-IDA (Fig. 2). The corresponding dissociation constants (Table 1) were almost 10-fold higher than those determined for the complexation of Zn(II), the natural metal ion in carbonic anhydrase II, or Zn(II)-IDA [13]. In the presence of NTA, no binding of Ni(II) to RBP/H_3(A) was detected (data not shown). The same observation had been made for Zn(II) previously [13]. Thus, the grafted metal-binding site in RBP/H_3(A) displayed selectivity for Zn(II) in comparison with Ni(II) and Cu(II) and it appeared that all three metal ions were complexed in an octahedral coordination geometry with three sites occupied by the imidazole groups of the protein and three sites occupied either by solvent molecules or by the tridentate IDA ligand. In contrast, the tetradentate NTA ligand gave rise to competition for the metal ion and prevented its binding to the protein.

Previous experiments on the selective binding of transition-metal ions to carbonic anhydrase II revealed an ~10-fold diminished affinity for Ni(II) compared with Zn(II) [19]. This finding is in agreement with our observation for the grafted binding site in RBP/H_3(A). However, binding of Cu(II) to carbonic anhydrase II was approximately one order of magnitude stronger than that of Zn(II), although in the absence of a chelate ligand [19]. This differing selectivity may be explained by the preferential tetrahedral coordination of the metal ion in the active center of the enzyme. Studies on metal-ion selectivity were also described in another protein design study, where the metal-binding site of carbonic anhydrase was transferred to the β-sheet near the antigen-binding region of an antibody [20,21]. The so-called 'metallo-antibody' was shown to exhibit much weaker binding for Zn(II) than for Cu(II). Both affinities, however, were far lower than those determined for RBP/H_3(A). Interestingly, in a study where the metal-binding site of carbonic anhydrase was grafted on the combining site of a catalytic antibody, Zn(II) binding was detected with a K_d value of 1.54 μM, whereas no affinity could be measured for Cu(II) or Ni(II) [22].

Generally, isolated His residues in proteins show an increasing strength of interaction in the series Zn(II) < Ni(II) < Cu(II) when tested for their affinities in IMAC applications [5]. Therefore, the selectivity against Ni(II) and Cu(II) observed in the case of RBP/H_3(A) emphasizes the special properties of the structurally defined metal-binding site that was engineered in this protein. Remarkably, a second binding site for Cu(II) was found in RBP/H_3(A) (Table 1) that was also present in wild-type RBP (Fig. 2a). This Cu(II)-binding activity is most likely due to the pair of naturally occurring His residues at positions 142 and 170 in the polypeptide sequence [13], which are in close proximity in space [9].

Comparison of the metal-binding site with a His_6 tag

The introduction of several histidine residues, so-called 'His-tags', at the carboxyl or amino terminus of a polypeptide chain to allow purification via IMAC has

Figure 3

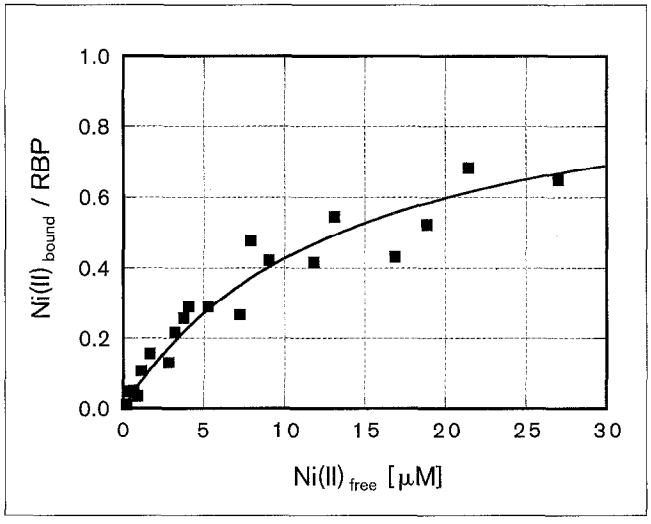

Metal-binding isotherms from equilibrium dialysis experiments with RBP/His_6 and Ni(II). The molar ratio of bound metal ion to protein is plotted against the concentration of free metal ion. The continuous line represents a least-squares fit as in Figure 2. The corresponding dissociation constant is given in Table 2. Ni(II) binding was measured at a protein concentration of 5.1 μM.

Table 2

Metal-binding properties of RBP/His_6 from equilibrium dialysis.

Metal ion	Stoichiometry	K_d [μM]
Zn(II)	2	3.6 ± 1.2; 1.9 ± 0.6[a]
Ni(II)	1	14.7 ± 1.3

[a]Data from [13]

become a popular method for isolation of recombinant proteins [23,24]. In order to determine the corresponding metal-binding properties, we used a variant of the recombinant wild-type RBP (i.e., without the metal-binding site of RBP/H_3(A)) that carried a His_6 tag (RBP/His_6) [14]. Equilibrium dialysis experiments were performed in the presence of Ni(II) and Ni(II)-IDA as above. For comparison, wild-type RBP without the His_6 tag (purified via the *Strep*-tag instead [13,15]) was also examined.

One specific binding site for Ni(II) on RBP/His_6 was found (Fig. 3), whereas no metal binding was detected for wild-type RBP without the tag. Interestingly, the presence of IDA led to a reduction in affinity of Ni(II) for the His_6 tag so that a K_d value could not be determined from the data within the Ni(II) concentration range investigated. Compared with the binding of Zn(II), which had been measured before [13], affinity for Ni(II) was about one order of magnitude weaker (Table 2). Furthermore, in the case of Zn(II) two binding sites had been observed for the His_6 tag. Their corresponding K_d values were similar and significantly lower than for the single Ni(II) binding site. This behavior reveals a distinct mechanism for complex formation between the structurally flexible His_6 tag and the two metal ions and contrasts with the stoichiometric properties of the rigid metal-binding site in RBP/H_3(A).

Synthesis and properties of a true 'IDA'-Sepharose

The observation that the transition-metal ions Zn(II) and Ni(II) are capable of being complexed by the metal binding site of RBP/H_3(A) and by another tridentate ligand at the same time prompted us to attempt the purification of RBP/H_3(A) from the bacterial protein extract by means of IMAC. When commercially available IDA attached to a Sepharose matrix (Chelating Sepharose Fast Flow, Pharmacia) was used, RBP/H_3(A) could be purified under carefully optimized conditions [13]. However, the separation showed surprisingly poor resolution, preventing the use of an imidazole step gradient for elution and thus limiting the practical application of this approach.

We assumed that this unexpected behavior was a result of the immobilization procedure employed during manufacturing of the IDA-Sepharose, where IDA is directly coupled to the epoxy-activated polymer [16]. The resulting product **1** (Fig. 1) has a third alkyl substituent at the IDA nitrogen with a hydroxy group in the β-position [16]. The association constant of the corresponding soluble compound, N-2-hydroxyethyl-iminodiacetic acid, for complex formation with transition-metal ions is more than one order of magnitude larger than that of free IDA [25], indicating that the β-hydroxy group acts as a fourth coordination center. Indeed, in the crystal structure of its Ni(II) complex [26] four coordination sites are occupied by the two carboxylates, the nitrogen, and the β-hydroxy group, with the two remaining positions in the octahedral coordination shell of Ni(II) occupied by water molecules. Therefore, not only steric hindrance by the third N-alkyl substituent but also competition of the tetradentate ligand with RBP/H_3(A) for the bound metal ion has to be taken into account; this is similar to the situation with NTA.

We therefore attempted to immobilize the IDA group at the Sepharose resin using an aliphatic substituent that emanated from one of its methylene groups, instead. For this purpose, N^{α}-carboxymethyl-(L)-lysine (NCL) (compound **3**) was synthesized [27] and linked by reacting the primary N^{ϵ}-amino group with Sepharose that had been activated with 4-nitrophenyl chloroformate [28]. A similar procedure was previously employed in the synthesis of NTA-agarose (compound **2**) [17]. Despite good coupling efficiency, the resulting matrix showed only weak binding

Figure 4

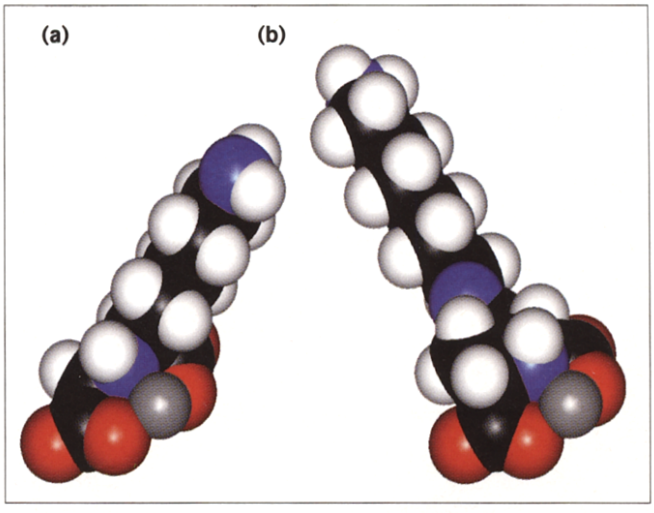

Van-der-Waals surface representations for **(a)** NCL (compound **3**) and **(b)** PDC (compound **4a**) (coupled to diaminohexane via a secondary amine), both in complex with a divalent metal ion (shown in grey). In the sterically preferred conformation of the NCL complex the linker substituent that emanates from one of the methylene groups of the IDA moiety points forward so that there is not enough room for a larger molecule to contact the metal ion. Cyclization of the IDA moiety in PDC results in a conformation such that the linker substituent points away from the metal. The molecules were generated with the program package INSIGHT II/DISCOVER (Biosym Technologies, Inc., San Diego, CA) and represent an energy-minimized conformation in the esff force field. (C: black; H: white; N: blue; O: red).

Figure 5

Reaction between N-(1-carboxyethylidene)-glycinatozinc(II) (compound **5**) and acroleine (compound **6**) to yield 3(4)-formyl-2-methylpyrrolidine-2,5-dicarboxylatozinc(II) (compound **4a**).

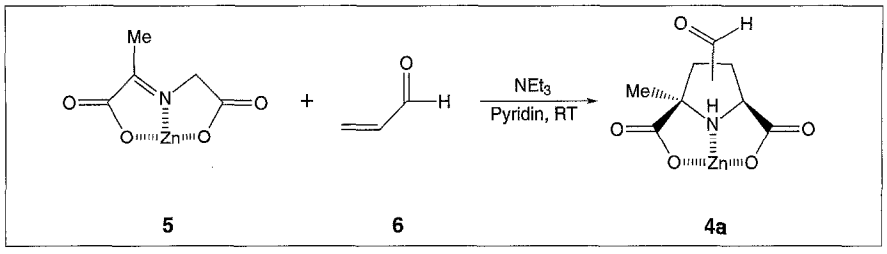

for Zn(II), which was quickly washed out when water was applied to the resin under chromatography conditions. It was possible to charge the column with Ni(II), which became complexed at a capacity of 4.3 μmol ml^{-1} NCL-Sepharose. However, the resin could not be successfully used for protein purification as RBP/H_3(A) was already eluted in the flow-through (data not shown).

A model of the ligand suggested (Fig. 4a) that the substituent at one of the methylene groups influenced the conformation of the IDA moiety such that the energetically favored conformation of the chelate ligand did not leave enough space for the simultaneous binding of the three bulky imidazole groups from the protein. To force the IDA moiety into a conformation which is structurally competent in this respect, cyclization appeared to be a promising approach (Fig. 4).

Synthesis of PDC as an alternative resin ligand

Derivatives of pyrrolidine-(*R,S*)-dicarboxylic acid (PDC) (compound **4**, Fig. 1) seemed to be suited for the formation of a relatively stable ternary complex with RBP/H_3(A) and a central metal ion. For the proper stereochemical arrangement of the two carboxylate groups in such a ligand, we used a synthesis based on the tendency of transition-metal complexes of imines derived from α-oxo acids and glycine to undergo stereospecific cycloaddition with electronegative olefins [29,30]. In the first step, an imine was formed from pyruvate and glycine that precipitated upon addition of Zn(II) acetate giving N-(1-carboxyethylidene)glycinatozinc(II) (compound **5**) in high yield (Fig. 5). This metallo-1,3-dipolar intermediate was used in a 4π + 2π cycloaddition with acroleine (compound **6**) under basic conditions, yielding 3(4)-formyl-2-methylpyrrolidine-2,5-dicarboxylatozinc(II) (compound **4a**) (95 %). This PDC derivative was obtained as a mixture of two regioisomers in respect to the position of the formyl group at a ratio of 4:1 C4-epimer:C3-epimer, as calculated from the integrals of the aldehyde proton peaks in ^1H NMR. The formyl group was useful for coupling the ligand to the gel matrix. As it was unlikely to interfere with the metal complexation in either of the different possible isomers (cf. Fig. 4b) no attempt was made to separate them. For immobilization to the gel

Figure 6

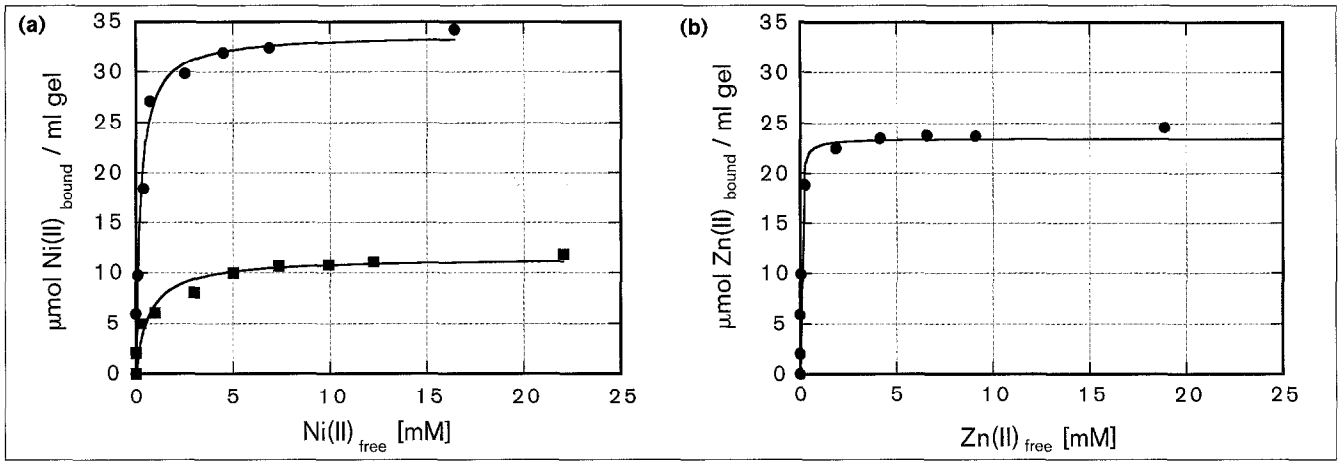

Adsorption isotherms for the binding of **(a)** Ni(II) to IDA-Sepharose (circles) and PDC-Sepharose (squares) and **(b)** for Zn(II) to IDA-Sepharose (circles). The amount of bound metal ion per volume wet gel is plotted against the concentration of free metal ion. The continuous lines represent least-squares fits according to the equation given in Materials and methods. The corresponding apparent dissociation constants and metal-ion capacities of the different resins are summarized in Table 3.

Table 3

Metal-binding properties of IDA- and PDC-Sepharose.

Metal ion	Chromatography resin	K_d (μM)	Metal-ion capacity (μmol ml^{-1} wet gel)
Zn(II)	IDA-Sepharose[a]	31 ± 5.2	23.4 ± 0.51
Ni(II)	IDA-Sepharose[a]	235 ± 65	33.7 ± 1.57
Ni(II)	PDC-Sepharose	662 ± 237	11.4 ± 0.66

[a]Commercial material from Pharmacia.

matrix, Sepharose CL-4B was activated with 4-nitrophenyl chloroformate [28]. After reaction of the activated Sepharose with excess 1,6-diaminohexane, the formyl group of PDC was coupled to the free amino groups, followed by reduction of the Schiff base with sodium cyanoborohydride.

Adsorption isotherms for the binding of Zn(II) and Ni(II) to the PDC-Sepharose were determined and compared with the commercially available IDA-Sepharose (Fig. 6). The PDC resin had a slightly higher dissociation constant for the binding of Ni(II) (Table 3), whereas the complexation of Zn(II) was too weak for proper evaluation. Binding studies performed under chromatography conditions showed that all of the Zn(II) that was applied to the PDC resin was quickly washed out. In contrast, Zn(II) bound to IDA-Sepharose even more strongly than did Ni(II), indicating an important function for the additional hydroxy group (see above). In the case of Ni(II), the PDC-Sepharose showed a binding capacity (Table 3) that was sufficient to perform chromatography experiments with a protein.

Use of PDC-Sepharose for IMAC of RBP/H_3(A)

IMAC was performed by applying periplasmic cell extract from *E. coli* containing RBP/H_3(A) to PDC-Sepharose charged with Ni(II). After unbound protein had been washed off, a linear concentration gradient of imidazole was applied. RBP/H_3(A) eluted at 180 mM imidazole whereas all non-specifically bound proteins eluted at a much lower concentration (Fig. 7). For comparison, the same experiment was carried out using IDA-Sepharose; in this case 40 mM imidazole was sufficient to elute RBP/H_3(A) under the same conditions (Fig. 7a) [13]. As binding of the contaminating bacterial proteins was not much different for the two resins (Fig. 7d), the separation of RBP/H_3(A) with immobilized PDC/Ni(II) appeared to be significantly more specific, making the use of an imidazole step gradient practical. When recombinant wild-type RBP was applied as a control, it was not specifically retarded by the column (data not shown). Thus, an efficient purification of RBP/H_3(A) from the bacterial protein extract was achieved with the PDC-Sepharose in a single step. This finding was in accordance with our structural model of the complex of RBP/H_3(A), Ni(II) and the PDC ligand (Fig. 8).

Figure 7

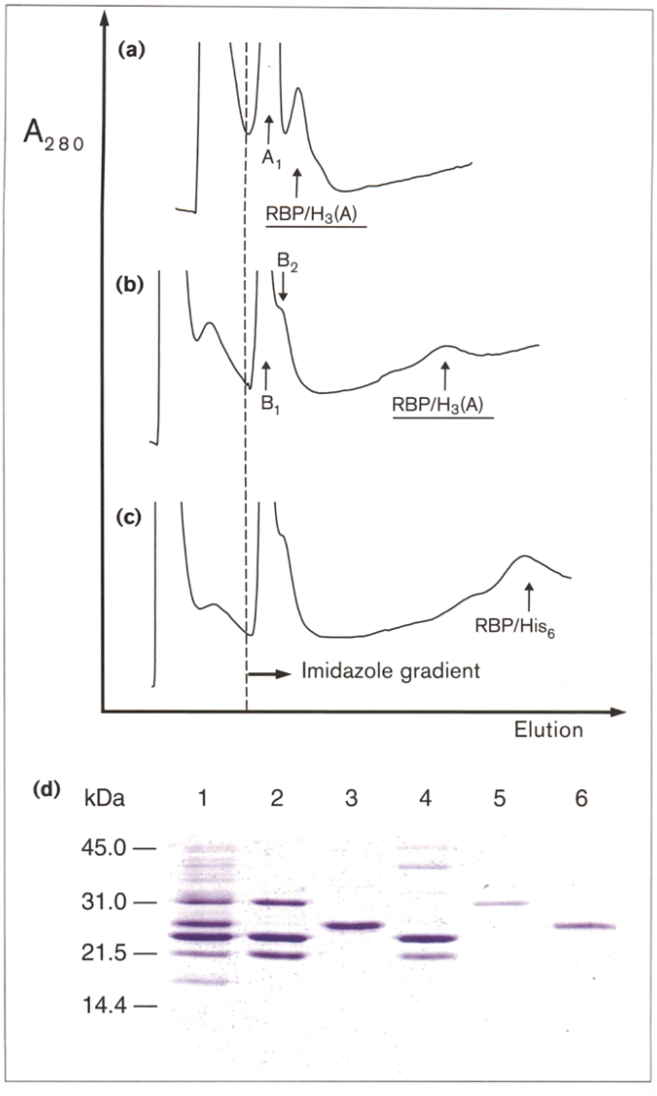

IMAC purification of RBP/H_3(A) and RBP/His_6 from a bacterial cell extract (periplasmic fraction). The elution profiles were aligned according to the imidazole gradients whose onset is at the dashed line. **(a)** Elution profile of RBP/H_3(A) using IDA-Sepharose ('Chelating Sepharose Fast Flow', Pharmacia). **(b)** Elution profile of RBP/H_3(A) using PDC-Sepharose. Due to the very flat gradient, which was used for keeping comparable conditions with the chromatogram in (a), the late elution of RBP/H_3(A) appeared broadened, although the yield remained unchanged. **(c)** Elution profile of RBP/His_6 using PDC-Sepharose. **(d)** SDS-PAGE of characteristic fractions from the chromatograms in (a) and (b). Lane 1: periplasmic protein fraction; 2: non-specifically bound fraction A_1; 3: RBP/H_3(A) from (a); 4: non-specifically bound fraction B_1; 5: non-specifically bound fraction B_2; 6: RBP/H_3(A) from (b). The fractions from the profile in (c) appear similar to those from the profile in (b) and were therefore omitted.

Given the improved performance of the PDC-Sepharose, we attempted to use it to purify a protein carrying a His_6 tag. A periplasmic cell extract containing RBP/His_6 was loaded onto a PDC-Sepharose column charged with Ni(II) under the same conditions as above. RBP/His_6 eluted at 250 mM imidazole (Fig. 7c). As the affinity of Ni(II) towards the His_6

tag is much weaker than towards RBP/H_3(A) (Tables 1,2), this surprising observation indicates once again that the steric requirements and energetics of metal-ion binding to the residues of the protein and to the chelate group of the immobile phase are delicately balanced, and that this balance is a critical determinant of the separation performance in IMAC. Altogether, PDC-Sepharose provides a resin with advanced properties for the purification of engineered proteins via IMAC.

Significance

The construction of artificial metal-binding sites in proteins was the first example of successful protein design and has therefore attracted special attention. The grafted Zn(II) binding site in RBP/H_3(A) is remarkable as it consists of only three His sidechains (with no requirement for cysteine residues) in an open and solvent-exposed manner, and yet it still exhibits one of the best affinities for metals realized among engineered proteins so far. Moreover, it displays selectivity against Cu(II) and Ni(II), as was demonstrated here.

This behavior contrasts with previous observations during IMAC purification of natural and engineered proteins, where the strength of metal ion affinity generally increases from Zn(II) to Ni(II) to Cu(II). Employing the RBP/His_6 variant, the Ni(II)-binding properties of a His_6 tag were now determined for the first time. In contrast to Zn(II), where two metal ions are complexed by each tag, only one Ni(II) ion is bound and with an even weaker affinity. In addition, the affinity for Ni(II) was reduced in the presence of IDA. These findings cannot easily be interpreted in structural terms and are particularly surprising in the light of the many successful applications of flexible His_6 tags in recombinant protein purification.

In the case of the structurally well defined metal binding site of RBP/H_3(A), however, it was possible to rationally design a metal chelate ligand that could form a complex with the metal and the protein. A substituted pyrrolidine-dicarboxylic acid was synthesized, which permitted, in its immobilized form, the purification of RBP/H_3(A) with as yet unachieved specificity, thus offering a considerable advantage in experimental applications. This behavior is in agreement with the notion that Ni(II) is sandwiched between the protein and the chelate ligand (see Fig. 8). The grafting of the same metal binding site to other proteins with exposed β-sheets should also be possible.

The construction of the metal binding site in RBP/H_3(A) and the design of a cognate metal chelate ligand constitute an example in which the engineering of a protein can be extended to include supra-molecular design, which may have further practical implications.

Figure 8

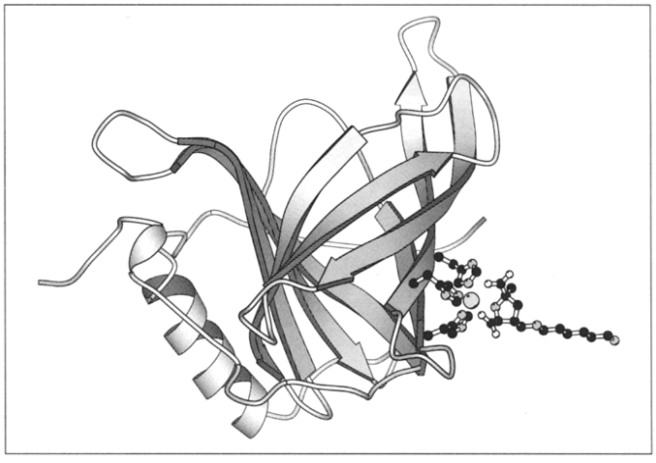

Structural model for the retinol-binding protein with the engineered metal-binding site, RBP/H_3(A), and the supra-molecular metal chelate interaction with Ni(II) and PDC. The metal ion possesses an approximately octahedral coordination sphere in which each of the three His residues from the protein occupies one coordination site. The tridentate pyrrolidine-dicarboxylic acid ligand (PDC (compound **4a**), as a secondary amine linked to the chromatography matrix with diaminohexane) occupies the three remaining coordination sites with its ring nitrogen atom and two carboxylate oxygens. The backbone of RBP/H_3(A) is depicted in a ribbon representation using the program MolScript [35] (C: black; N: grey; O: white; metal ion: grey sphere; H: *not shown*).

Materials and methods

Equilibrium dialysis

Equilibrium dialysis with purified RBP/H_3(A), RBP/His_6, or wild-type RBP was performed in small acrylic chambers as described [13], using KSH buffer (50 mM K_2SO_4, 20 mM N-(2-hydroxyethyl)piperazine-N'-2-ethane-sulfonic acid/KOH pH 7.5) both for the protein and the metal salts ($CuCl_2$ or $NiCl_2$). For each data point 400 μl of protein solution (with RBP/H_3(A) concentrations in the range of 2–10 μM, see Figure legends) was equilibrated overnight at 22 °C against an equal volume of metal-ion solution (with concentrations ranging from 1–20 μM for $NiCl_2$, $CuCl_2$, and Ni(II)-IDA, from 0–10 μM for Ni(II)-NTA and from 0–12 μM for Cu(II)-IDA). The metal-ion concentration in the two chambers was then determined by atomic absorption spectrometry in a pyrolyzed graphite tube with L'vov platform using an AS5000 instrument with the furnace atomizer system HGA500 (Perkin Elmer GmbH, Überlingen, Germany) according to the manufacturer's recommendations. The samples were applied with the automatic sampler AS40, dried (15 s at 90 °C and 20 s at 120 °C) and ashed (20 s at 1200 °C for Cu(II), 1400 °C for Ni(II)). The atomic absorption during atomization (8 s at 2300 °C for Cu(II), 4 s at 2500 °C for Ni(II)) was measured at 324.8 nm for Cu(II) with the bandwidth set to 0.7 nm and at 232 nm for Ni(II) with the bandwidth set to 0.2 nm. For the calibration of the spectrophotometer, gravimetrically prepared solutions of Cu(II)-IDA and Ni(II)-IDA served as standards. Each sample was measured three times and the mean value was calculated and recorded automatically. The analysis of binding data and calculation of affinity constants was carried out using the mathematical procedures and formula as described [13]. For metal-binding experiments in the presence of IDA or NTA, complexes of Cu(II) or Ni(II) with these chelate ligands were prepared by mixing aqueous stock solutions containing equimolar amounts of recrystallized IDA [13] or NTA and $CuCl_2$ or $NiCl_2$, respectively. In order to complex trace amounts of metal ions originating from the buffer substances, the chelator compounds were also added to the protein solution at a concentration

of 2 μM. For the quantification of Ni(II) concentrations in experiments that were performed in the absence of IDA or NTA, 100 μM ethylenediamine tetraacetic acid (EDTA) was added prior to the measurement in order to obtain reproducible results.

Synthesis of NCL

The synthesis of N^{α}-carboxymethyl-(L)-lysine was carried out essentially as described [27]. ^{1}H-NMR spectra were recorded on a Bruker 300 MHz instrument using tetramethylsilane as an internal standard. δ (D_2O) 1.50 (m, 2H; $^{\delta}CH_2$), 1.73 (m, 2H; $^{\gamma}CH_2$), 1.95 (m, 2H; $^{\beta}CH_2$), 3.03 (t, 2H; $^{\epsilon}CH_2$), 3.60 (dd, 2H; $^{\alpha'}CH_2$), 3.71 (t, 1H; $^{\alpha}CH$).

Synthesis of formyl-methyl-PDC

For the synthesis of N-(1-carboxyethylidene)glycinatozinc(II) (compound **5**) [29,30], 7.5 g glycine (100 mmol) was suspended in 20 ml 33 % (v/v) aqueous ethanol at room temperature and 7.0 ml pyruvic acid (100 mmol) was added. The mixture was stirred until a homogeneous solution was obtained (~30 min). 22.0 g zinc acetate • 2 H_2O (100 mmol) dissolved in 140 ml 33 % (v/v) aqueous ethanol was then added and the mixture was stirred at room temperature for 4 h. The precipitated metal complex **5** was collected by suction filtration and dried *in vacuo* over P_4O_{10}. ^{1}H NMR: δ (D_2O) 2.28 (s, 3H, Me) and 4.12 (s, 2H, CH_2). For the synthesis of 3(4)-formyl-2-methylpyrrolidine-2,5-dicarboxylatozinc(II) (compound **4a**), 2.1 g of the product **5** (10 mmol) was suspended in 100 ml dry degassed pyridine. 1.40 ml triethylamine (10 mmol) and 663 μl acroleine (10 mmol) were then added with stirring. After stirring for 48 h at room temperature, the solvent was removed at 45 °C under reduced pressure. For complete removal of pyridine, the remainder was dissolved three times in 20 ml 25 % (v/v) aqueous ethanol, which was then again evaporated. The residual oil was dissolved in a few ml water and the cycloadduct was precipitated by the addition of ethanol. The colorless crystals were collected by suction filtration and dried *in vacuo* over P_4O_{10}. Two regioisomers with the aldehyde group at different positions were distinguishable by ^{1}H NMR: δ (D_2O) C-3 epimer: 1.72 (s, 3H, ^{2}Me), 2.34 (m, 2H, $^4CH_2$), 3.07 (m, 1H, ^{3}H), 4.02 (dd, 1H, ^{5}H), 5.20 (d, 1H, CHO); C-4 epimer: 1.52 (t, 3H, ^{2}Me), 2.57 (m, 2H, $^3CH_2$), 2.93 (m, 1H, ^{4}H), 3.95 (d, 1H, ^{5}H), 5.14 (d, 1H, CHO). For each epimer only one diastereomer was detected.

Coupling of NCL and PDC to Sepharose

Activation of Sepharose CL-4B (Pharmacia, Freiburg) was performed using 20 ml of 200 mM *p*-nitrophenyl chloroformate and 20 ml 350 mM 4-dimethylaminopyridine for 10 ml of wet, sedimented Sepharose gel [29]. The yield of activation was estimated by absorption measurement at 400 nm after hydrolysis of an aliquot of the gel with NaOH. For the coupling of NCL, 4 ml of an aqueous solution of 50 mM NCL/NaOH pH 10.0 was added to 4 ml (wet volume) of the activated resin and incubated over night with gentle agitation. For the coupling of PDC, 4 ml of 3 M diaminohexane/HCl pH 10.0 was first added to 4 ml of the activated resin. The mixture was incubated overnight at room temperature with gentle agitation. The gel was then washed on a sintered glass funnel with excess water, followed by 100 mM acetic acid/100 mM NaCl pH 5.0, water, and 100 mM sodium borate pH 8.5. After the addition of 4 ml 500 mM PDC in 100 mM sodium borate pH 8.5 the gel was incubated for 3 h with agitation. Then 1 ml of 6 M sodium cyanoborohydride was added and the mixture was incubated for another 20 h. Finally, the resin was washed with excess water.

Metal-binding properties of the chromatography resins

200 μl of an aqueous suspension of derivatized Sepharose (containing 100 μl drained gel, devoid of bound metal ions) was mixed with 200 μl aliquots of 1, 3, 5, 10, 15, 20, 25, 30 or 50 mM aqueous $NiCl_2$ or $ZnSO_4$ solutions, respectively. Each mixture was incubated at room temperature for 60 min and resuspended several times. After centrifugation of the gel the concentration of unbound Ni(II) was measured by mixing 250 μl from the supernatant with 150 μl water and 100 μl 0.5 M EDTA pH 8.5. The concentration of Ni(II) was determined from the absorption of the EDTA complex at 1000 nm using an extinction coefficient $\epsilon = 31.1\ M^{-1}cm^{-1}$. To measure the concentration of unbound Zn(II), aliquots from each supernatant were diluted such that the maximum concentration did not exceed 50 μM. 400 μl of each of these samples was mixed with 340 μl water, 200 μl 0.2 M potassium phthalate pH 9.0 and 60 μl 2 mM zincon (Sigma) in 2 mM NaOH. The concentration of Zn(II) was then determined from the absorption of the zincon complex at 625 nm with $\epsilon = 11\ 890\ M^{-1}\ cm^{-1}$. Calculation of the metal-binding capacity $[Me(II)^{max}_{bound}]$ and of the apparent dissociation constant K_d were performed by non-linear regression of the equation

$$[Me(II)_{bound}] = \frac{[Me(II)^{max}_{bound}]}{1 + \frac{K_d}{[Me(II)_{free}]}}$$

whereby $[Me(II)_{bound}]$ was determined as the difference between the total metal-ion concentration and the measured concentration of metal ion in the supernatant, $[Me(II)_{free}]$, calculated for the drained gel volume.

Immobilized metal affinity chromatography (IMAC)

Expression of the RBP variants was carried out in a 2-l culture of *E. coli* JM83 harboring an appropriate derivative of the expression vector pASK75 [31,32], together with pASK61 [13,14]. After 3 h induction with anhydrotetracycline [31] the periplasmic cell fraction was prepared and dialyzed against CP buffer (1 M NaCl, 0.04 M Na phosphate pH 7.5). IMAC was then performed on a column (78.5 mm^2 x 51 mm) containing 4 ml of freshly prepared chromatography resin charged with Ni(II). After equilibration with CP buffer, 15 ml of periplasmic cell fraction corresponding to 1 l *E. coli* culture was applied (flow rate 38.0 ml h^{-1}). The column was washed with CP buffer until absorption at 280 nm (A_{280}) of the flow-through reached the baseline. Then a linear gradient (360 ml) from 0 to 300 mM imidazole in CP buffer (pH 7.5) was applied. Eluted protein fractions were analyzed by 15 % SDS-PAGE [33].

Modelling of the trimolecular complex

Modelling of the structure shown in Fig. 8 was based on the crystal structure of RBP [9], in which the amino acids at positions 46, 54 and 56 were replaced by a corresponding structural set of the three His sidechains and the bound Zn(II) ion from the active center of carbonic anhydrase II [12] as described for RBP/H_3(A) [13]. To model the ternary complex with compound **4a** the crystal structure of the Ni(II)-IDA complex [34] was used. In this structure the Ni(II) ion was octahedrally liganded by a combination of the nitrogen atom, the two carboxymethyl groups of IDA and three water molecules. Using the program package INSIGHT II/DISCOVER (Biosym Technologies, Inc., San Diego, CA) the positions of the oxygen atoms of these water molecules and of the Ni(II) ion were optimally superimposed on the complexing nitrogen atoms of the three His residues and the Zn(II) ion in the binding site of RBP/H_3(A). The water molecules and the Zn(II) ion were then deleted. The resulting position and conformation of the IDA group was the starting point for the modeling of PDC **4a** from a cyclopentane standard conformation, including a diaminohexane linker bound via a secondary amine. Standard bond lengths and angles were used and the structure was finally energy minimized in a force-field calculation.

Acknowledgements

This work was supported by a grant from the Deutsche Forschungsgemeinschaft to A.S. and a Kekulé studentship from the Fonds der Chemischen Industrie to A.M.S.

References

1. Regan, L. (1995). Protein design: novel metal-binding sites. *Trends Biochem. Sci.* **20**, 280–285.
2. Kellis, J.T., Jr., Todd, R.J. & Arnold, F.H. (1991). Protein stabilization by engineered metal chelation. *Biotechnology* **9**, 994–995.

3. Regan, L. & Clarke, N.D. (1990). A tetrahedral zinc(II)-binding site introduced into a designed protein. *Biochemistry* **29**, 10878–10883.
4. Handel, T. & DeGrado, W.F. (1990). *De novo* design of a Zn^{2+}-binding protein. *J. Am. Chem. Soc.* **112**, 6710–6711.
5. Arnold, F.H. (1991). Metal-affinity separations: a new dimension in protein processing. *Biotechnology* **9**, 151–156.
6. Arnold, F.H. & Haymore, B.L. (1991). Engineered metal-binding proteins: purification to protein folding. *Science* **252**, 1796–1797.
7. Soprano, D.R. & Blaner, W.S. (1994). Plasma retinol-binding proteins. In *The Retinoids: Biology, Chemistry, and Medicine.* (2nd edn) (Sporn, M.B., Roberts, A.B. & Goodman, D.S., eds), pp. 257–281, Raven Press, New York.
8. Newcomer, M.E., *et al.*, & Peterson, P.A. (1984). The three-dimensional structure of retinol-binding protein. *EMBO J.* **3**, 1451–1454.
9. Cowan, S.W., Newcomer, M.E. & Jones, T.A. (1990). Crystallographic refinement of human serum retinol-binding protein at 2 Å resolution. *Proteins* **8**, 44–61.
10. Zanotti, G., Ottonello, S., Berni, R. & Monaco, H.L. (1993). Crystal structure of the trigonal form of human plasma retinol-binding protein at 2.5 Å resolution. *J. Mol. Biol.* **230**, 613–624.
11. Eriksson, A.E., Jones T.A. & Liljas, A. (1988). Refined structure of human carbonic anhydrase II at 2.0 Å resolution. *Proteins* **4**, 274–282.
12. Eriksson, A.E., Kylsten, P.M., Jones, T.A. & Liljas, A. (1988). Crystallographic studies of inhibitor binding sites in human carbonic anhydrase II: a pentacoordinated binding of the SCN^- ion to the zinc at high pH. *Proteins* **4**, 283–293.
13. Müller, H.N. & Skerra, A. (1994). Grafting of a high-affinity Zn(II)-binding site on the β-barrel of retinol-binding protein results in enhanced folding stability and enables simplified purification. *Biochemistry* **33**, 14126–14135.
14. Müller, H.N. & Skerra, A. (1993). Functional expression of the uncomplexed serum retinol-binding protein in *Escherichia coli*: ligand binding and reversible unfolding characteristics. *J. Mol. Biol.* **230**, 725–732.
15. Schmidt, T.G.M. & Skerra, A. (1994). One-step affinity purification of bacterially produced proteins by means of the '*Strep*-tag' and immobilized recombinant core streptavidin. *J. Chromatogr. A* **676**, 337–345.
16. Porath, J., Carlsson, J., Olsson, I. & Belfrage, G. (1975). Metal chelate affinity chromatography, a new approach to protein fractionation. *Nature* **258**, 598–599.
17. Hochuli, E., Döbeli, H. & Schacher, A. (1987). New metal chelate adsorbent selective for proteins and peptides containing neighbouring histidine residues. *J. Chromatogr.* **411**, 177–184.
18. Matthews, D.J. & Wells, J.A. (1994) Engineering an interfacial zinc site to increase hormone–receptor affinity. *Chemistry & Biology* **1**, 25–30.
19. Lindskog, S. & Nyman, P.O. (1964). Metal-binding properties of human erythrocyte carbonic anhydrases. *Biochim. Biophys. Acta* **85**, 462–474.
20. Iverson, B.L., *et al.*, & Lerner, R.A. (1990). Metalloantibodies. *Science* **249**, 659–662.
21. Wade, W.S., Koh, J.S., Han, N., Hoekstra, D.M. & Lerner, R.A. (1993). Engineering metal coordination sites into the antibody light chain. *J. Am. Chem. Soc.* **115**, 4449–4456.
22. Stewart, J.D., Roberts, V.A., Crowder, M.W., Getzoff, E.D. & Benkovic, S.J. (1994). Creation of a novel biosensor for Zn(II). *J. Am. Chem. Soc.* **116**, 415–416.
23. Hochuli, E., Bannwarth, W., Döbeli, H., Gentz, R. & Stüber, D. (1988). Genetic approach to facilitate purification of recombinant proteins with a novel metal chelate adsorbent. *Biotechnology* **6**, 1321–1325.
24. Skerra, A., Pfitzinger, I. & Plückthun, A. (1991). The functional expression of antibody F_v fragments in *Escherichia coli*: improved vectors and a generally applicable purification technique. *Biotechnology* **9**, 273–278.
25. Martell, A.E. & Smith, R.M. (1974). N-(2-hydroxyethyl)iminodiacetic acid (HIDA). In *Critical Stability Constants, Vol. 1*, p. 165, Plenum Press, New York and London.
26. Polyakova, I.N., Polynova, T.N. & Porai-Koshits, M.A. (1981). Crystal structure of nickel(II) β-hydroxyethyliminediacetate trihydrate. *Koord. Khim.* **7**, 1894.
27. Kihlberg, J., Bergman, R. & Wickberg, B. (1983). Synthesis of strombine. A new method for monocarboxylation of primary amines. *Acta Chem. Scand. B* **37**, 911–916.
28. Bayer, E.A., Ben-Hur, H. & Wilchek, M. (1990). Isolation and properties of streptavidin. *Methods Enzymol.* **184**, 80–89.
29. Grigg, R., Sridharan, V. & Thianpatanagul, S. (1986). X=Y-ZH systems as potential 1,3-dipoles. Part 6. Metallo-1,3-dipoles. Cycloadditions of divalent metal complexes of glycine and alanine imines to electronegative olefins. *J. Chem. Soc. Perkin Trans. I*, 1669–1674.
30. Casella, L., Gullotti, M. & Melani, E. (1982). The reaction of copper(II) complexes of glycine imines with activated olefines. *J. Chem. Soc. Perkin Trans. I*, 1827–1831.
31. Skerra, A. (1994). Use of the tetracycline promotor for the tightly regulated production of a murine antibody fragment in *Escherichia coli*. *Gene* **151**, 131–135.
32. Müller, H.N. (1995). Konstruktion eines Lipocalins mit neuen Eigenschaften. Dissertation, University of Frankfurt, Frankfurt am Main, Germany
33. Fling, S.P. & Gregerson, D.S. (1986). Peptide and protein molecular weight determination by electrophoresis using a high-molarity Tris-buffer system without urea. *Anal. Biochem.* **155**, 83–88.
34. Agre, V.M., Sisoeva, T.F., Trunov, V.K., Dyatlova, N.M. & Fridman, A.Y. (1984). Crystal structure of dipotassium tris(iminodiacetato)-dinickelate hexahydrate. *Zh. Strukt. Khim.* **25**, 141–142.
35. Kraulis, P.J. (1991). MOLSCRIPT: a program to produce both detailed and schematic plots of protein structures. *J. Appl. Cryst.* **24**, 946–950.